64th meeting of Programme Advisory Committee for Particle Physics
JINR ICC, Dubna, 15 – 16 June, 2026

THERMOMETRY AND THERMAL STATUS OF THE MPD MAGNET TRIM COILS

M. Medvedeva[1,2], A. Fedotov[1], S. Movchan[1]
[1]Veksler and Baldin Laboratory of High Energy Physics, Joint Institute for Nuclear Research, Dubna, Russia
[2]Laboratory of Physics of Perspective Materials, Institute for Nuclear Problems of Belarusian State University, Minsk, Belarus

MOTIVATION

The Multi-Purpose Detector (MPD) at NICA experiment (JINR) is designed for tracking and identifying particles produced in heavy-ion collisions. Its magnet is based on a NbTi superconducting coil and an iron yoke for magnetic-flux return. The system is required to provide a central field of B_0 = 0.5 T within a 4.656 m aperture, enabling transverse-momentum reconstruction in the range 0.1–1 GeV/c [1,2].

In the MPD Time Projection Chamber (TPC), filled with the P10 working gas mixture, this magnetic-field configuration reduces transverse electron diffusion by approximately a factor of 6.7 compared with operation without a magnetic field. Therefore, the field quality is constrained both by the total spatial homogeneity δ and by the integral (radial) field distortion $\Im_r$ along the TPC drift direction (z) [1,2]:

$$\delta = \frac{\max\left(\left|\vec{B}\right|\right) - \min\left(\left|\vec{B}\right|\right)}{2B_0} \approx 10^{-3}, \qquad \Im_r = \int_{z}^{z_{max}} \left|\frac{B_r}{B_z}\right| dz \le 1.5 \text{ mm}.$$

Field non-uniformities originating from yoke asymmetry, local iron saturation, mechanical misalignments, or imperfections in the current distribution are difficult to compensate after assembly. In contrast, the correctable end-region component associated with the fringe field of the finite-length solenoid is compensated in MPD by axisymmetric resistive trim coils installed in dedicated recesses at the poles.

The MPD trim coils were custom-manufactured by ASG Superconductors [3,4] and are conventionally designated as the East (E) and West (W) units. Each coil consists of two adjacent insulated Archimedean spirals that are oppositely wound. The spirals are made of hollow copper conductor with an internal channel for coolant (water) circulation. The trim-coil Joule heat load must be limited because of the thermal sensitivity of the nearby TPC gas volume. Frontal thermal screens protect the TPC barrel end supports from heat produced by the trim coils and part of the Time-of-Flight detector (TOF); with an estimated TOF contribution of about 200 W per end and a screen capacity of 500 W, the allowable trim-coil heat load is Q^{max} = 300 W per end.

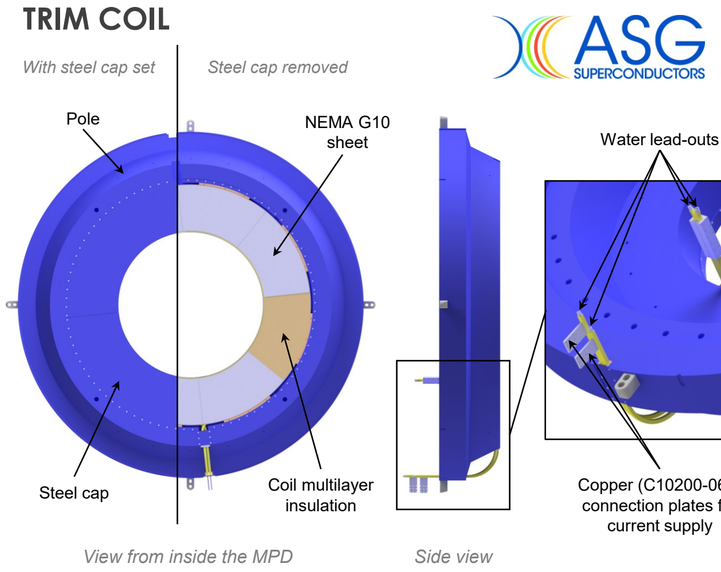
This study aimed to identify thermally stabilized operating regimes of the trim coils that minimize heat exchange with the surrounding air inside the MPD and, consequently, with nearby subdetectors. The main tasks were (i) to investigate the thermal behavior of the trim coils at these reference currents for different coolant inlet parameters and ambient conditions, (ii) to quantify the heat fluxes directed into the MPD inner volume, and (iii) to determine potentially critical regimes at and above the present reference currents. The currents denoted as nominal in the present work should be regarded as provisional and may be revised during further tuning and commissioning of the MPD magnet.

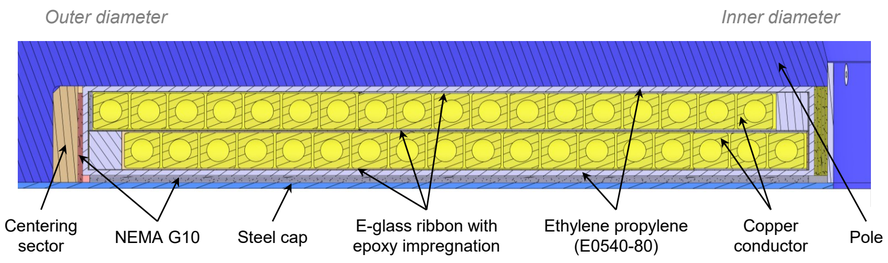
A three-dimensional finite-element model of the trim coil was developed in COMSOL Multiphysics for thermal simulations. A dedicated thermometry system was deployed for the MPD magnet, and the numerical model was verified against experimental temperature measurements and coolant outlet data with MAPE < 1.5%, confirming its suitability for predictive parametric studies.

[1] *V. M. Golovatyuk and V. D. Kekelidze, 'MPD: MultiPurpose Detector — Project Proposal 2020', JINR, Dubna, 2020.*
[2] *MPD Collaboration, 'Multi-Purpose Detector (MPD) Solenoid and Magnet Yoke: TDR', JINR, Dubna, 2019.*
[3] *ASG Superconductors, MPD Trim Coil & Pole Assembly Drawings, 2017.*
[4] *ASG Superconductors, 'Magnetic Calculation MPD Dubna rev.3', 2016.*

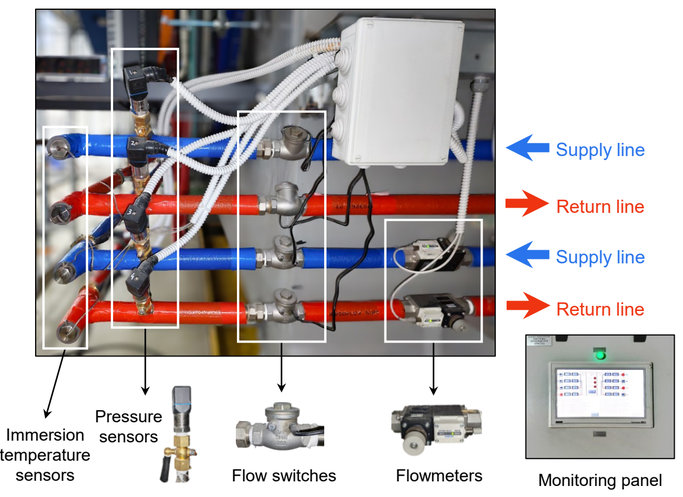
Acknowledgements: *S.Gerasimov, A. Bazhazhin, N. Bikmetov, D. Tereshin, K. Mukhin, A. Rybakov, M. Buryakov.*

TRIM COIL





COOLING SYSTEM



GEOMETRICAL & OPERATING PARAMETERS

Trim coil	West	East
Material & configuration	2 Archimedean copper spirals stacked; wound from the center; lead-outs at outer diameter	
Turns per coil	36	
Conductor cross-section	30×30 mm²	
Cooling channel diameter	19 mm	
Inner diameter d_{in}	1960 mm	
Outer diameter d_{out}	3180 mm	
Axial thickness	75 mm	
Mass	1.77 ton	
Power supply U	43 V	
Nominal current I	2688 A	2795 A
Maximum current I^{max}	4194 A	
Resistance R	8.2187 mΩ	8.1641 mΩ
Power loss P	59383 W	63778 W
Maximum power loss P^{max}	144564 W	143604 W
Coolant flow rate q	19 L/min	
Coolant inlet pressure p_{inlet}	2.3 atm	
Coolant outlet pressure p_{outlet}	0.7-0.9 atm	
Coolant inlet temperature T_{inlet}	18-22 °C	
Coolant outlet temperature threshold T_{outlet}^{max}	55 °C	
References	[1-4]	

PHYSICAL MODEL

3D Heat transfer in solids

Heat-conduction equation $-\nabla \cdot \left(k_s \nabla T_s\right) = S$

S – volumetric heat source included in the resistive trim coil ($S = \frac{P}{V}$) and omitted elsewhere ($S = 0$)
T_s – temperature of the solid domain
k_s – thermal-conductivity coefficient of the solid domain
P – source power associated with Joule dissipation in a conductor of volume V

1D Laminar channel flow (viscous, incompressible, non-isothermal fluid formulation)

Momentum transport $\frac{dp}{ds} = -\frac{f_D \rho}{2d_h} u|u|$,

Continuity equation $\frac{d}{ds}\left(A_h \rho u\right) = 0,\ A_h = \frac{\pi d_h^2}{4}$

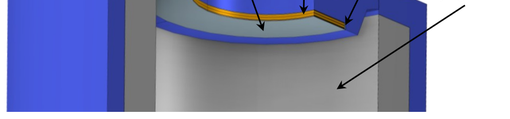
Heat transport $\rho A_h c_p u \frac{dT}{ds} = \frac{d}{ds}\left(A_h k \frac{dT}{ds}\right) + \frac{f_D \rho A_h}{2d_h} u^3 + h_{wall}\left(T_s - T\right)$

s – axial coordinate
p – pressure
u – cross-section averaged velocity
f_D – Darcy friction factor
d_h – hydraulic diameter
ρ – water density
μ – water dynamic viscosity
c_p – water specific heat capacity
k – water thermal conductivity
A_h – flow cross-sectional area
h_{wall} – effective linear heat-transfer coefficient between the coolant and the surrounding solid domains at temperature T_s

FINITE-ELEMENT MODEL

The West and East trim coils were analyzed separately.
- p, u, T → quadratic basis functions ($O(\Delta^2)$)
- T_s → linear basis functions ($O(\Delta)$)
- Solver relative tolerance 10^{-9}
- Discretization-independent results
- Mesh of about $3.7 \cdot 10^6$ elements
- Mesh-convergence tests demonstrated discretization-independent results

COMSOL MULTIPHYSICS



Cutaway of the computational domain

BOUNDARY CONDITIONS

Fixed flow rate & temperature: $u = \frac{q}{A}, T = T_{inlet}$

Heat outflow & fixed pressure: $p = p_{outlet}, \frac{dT}{ds} = 0$

The coolant circulation within the coil follows a counter-flow arrangement, with the coolant entering one spiral at the inner diameter and the other at the outer diameter.

Thermally thick approximation for the coil multilayer insulation

$$-\mathbf{n}_j \cdot \left(k_s \nabla T_s\right) = -\frac{\left(T_u - T_d\right)}{\sum_{i=1}^{N_{layers}} \frac{d_i}{k_i}},\ j = \overline{1, N}$$

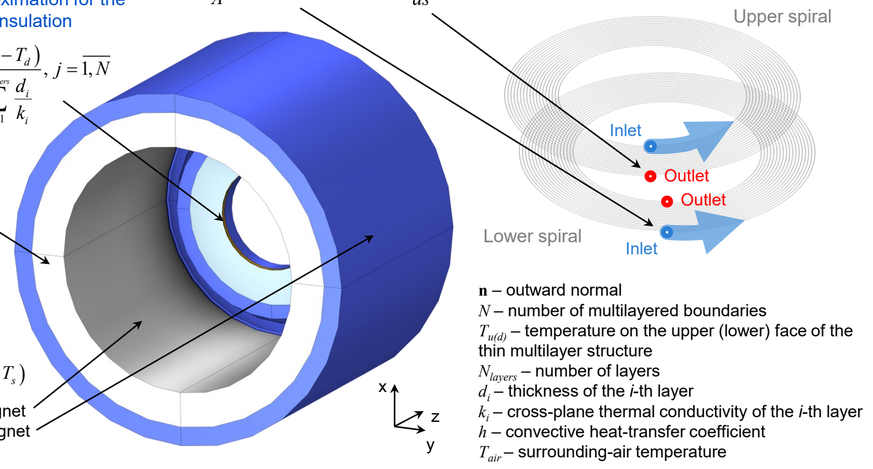
Adiabatic cut plane face

$$-\mathbf{n} \cdot \left(k_s \nabla T_s\right) = 0$$

Convective heat exchange with air

$$-\mathbf{n} \cdot \left(k_s \nabla T_s\right) = -h\left(T_{air} - T_s\right)$$

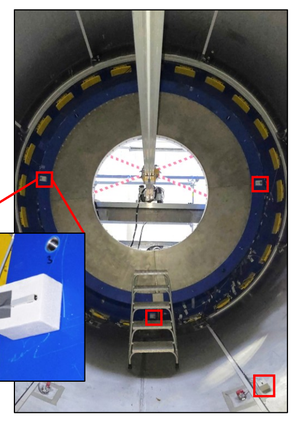
$T_{air} = T_{int}$ inside the magnet
$T_{air} = T_{ext}$ outside the magnet

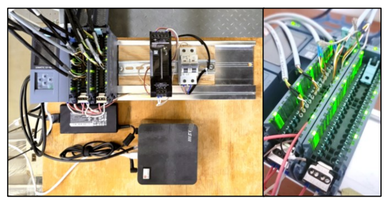


$\mathbf{n}$ – outward normal
N – number of multilayered boundaries
$T_{u(d)}$ – temperature on the upper (lower) face of the thin multilayer structure
N_{layers} – number of layers
d_i – thickness of the i-th layer
k_i – cross-plane thermal conductivity of the i-th layer
h – convective heat-transfer coefficient
T_{air} – surrounding-air temperature

THERMOMETRY SETUP

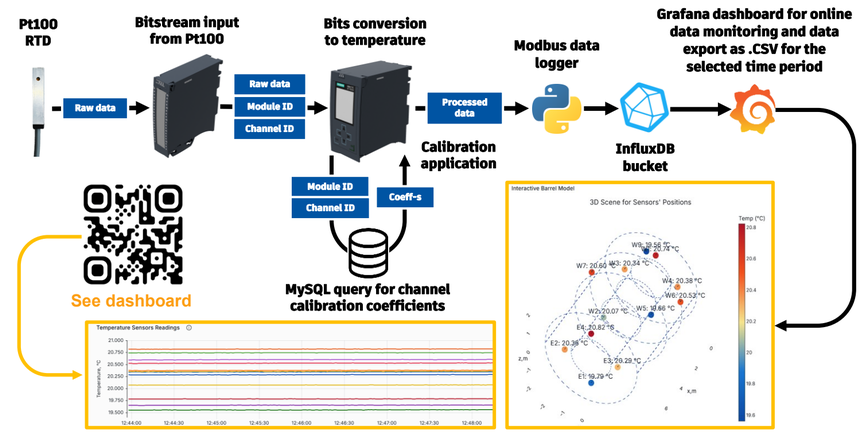
Control and data aggregation
Siemens S7-1515-2 PLC networked to MSI Cubi NUC M1 PC via Ethernet (IPv4).
Signal acquisition
AI 8xU/I/RTD/TC HF modules, resolution 0.001 °C/bit, 8 measurement channels, each supporting four-wire resistance measurements.
Channel calibration
Channel-to-channel offsets up to 0.2 °C within AI module motivated channel-wise calibration using Tonifishi Q10 programmable resistor box with stability up to 0.001 Ω (0.003 °C/channel).
Measuring equipment
Pt100-385 Class AA resistance thermometers with a room-temperature tolerance of ≈ 0.1 °C. Signals from Pt100 RTDs were transmitted to the AI modules over cables up to 30 m long.
Pt100 RTDs placement
2 sensors on the service platform → daily temperature variations in the MPD hall (T_{ext}).
12 sensors mounted on Penoplex© insulation → temperature of the internal air (T_{int}).
1 sensor without insulation → temperature of the West-coil steel cap.



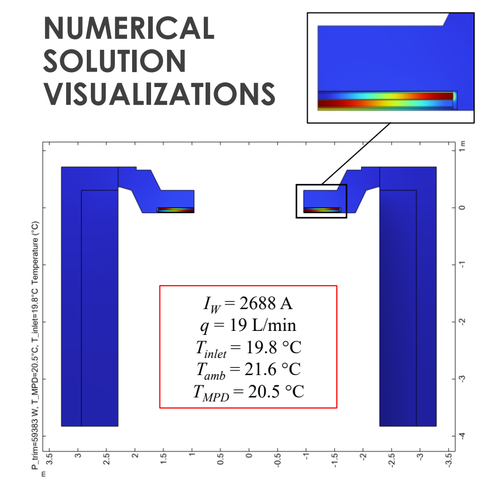


Thermometry hardware

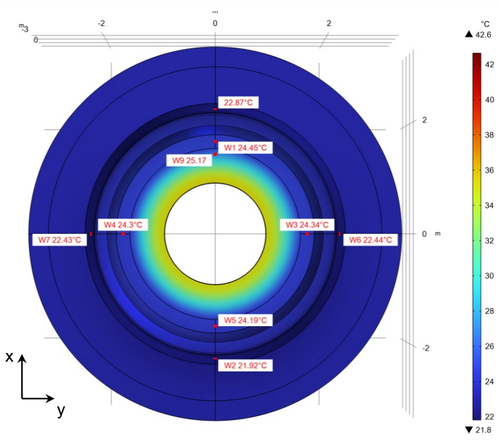
DATA EXCHANGE DIAGRAM FOR THERMOMETRY SOFTWARE



NUMERICAL SOLUTION VISUALIZATIONS



Water temperature in channels



West coil surface temperature with point markers at the Pt100 RTD locations

RESULTS OF NUMERICAL PARAMETRIC STUDIES

The simulations took into account the temperature gradient within the MPD volume:

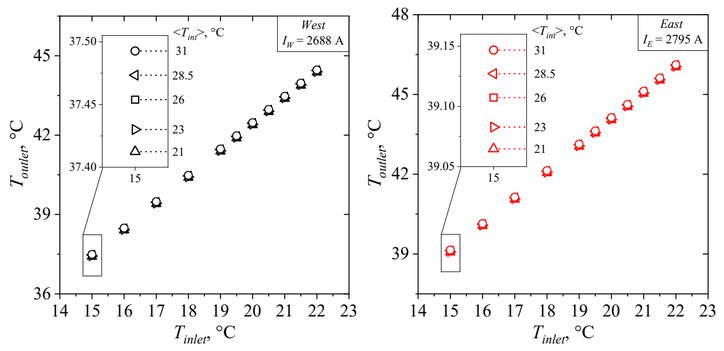
$$T_{int}(x) = T_{int}' + \frac{x + R_{in}}{2R_{in}} \cdot \Delta T_{int}$$

The integral heat flux was calculated numerically as

$$Q = \iint_A h\left(T_s - T_{int}\right) dA$$

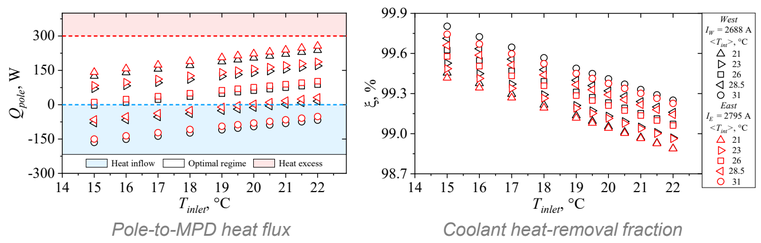
T_{int}' – reference temperature at the lower point of the pole
R_{in} – inner radius of the yoke
ΔT_{int} = 2 °C – temperature gradient amplitude
$\langle T_{int} \rangle$ – temperature at mid-height
A – inner surface area

Spiral notation: W1 – West lower (at the yoke recess bottom), W2 – West upper, E1 – East lower, E2 – East upper



Coolant outlet temperatures for W1 (left) and E1 (right) spirals

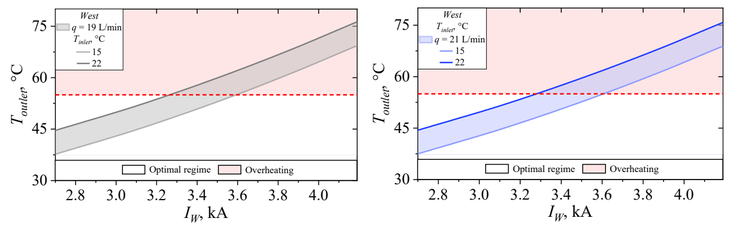
Currents (nominal)
I_W = 2688 A, I_E = 2795 A
Coolant inlet conditions per spiral
q = 19 L/min
T_{inlet} = 15-22 °C
Ambient conditions
T_{ext} = 21.6 °C
T_{int}' = 20-30 °C



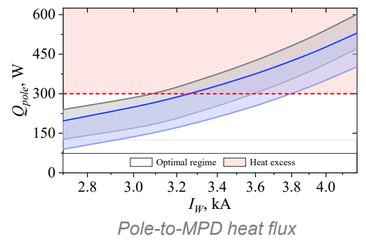
Pole-to-MPD heat flux

Coolant heat-removal fraction

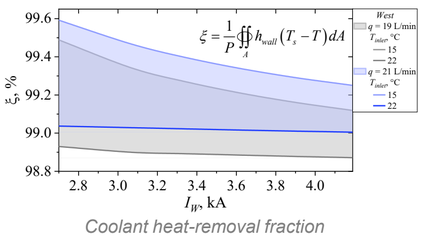
Currents (nominal-to-maximum)
I_W = 2688-4194 A
Coolant inlet conditions per spiral
q = 19, 21 L/min
T_{inlet} = 15-22 °C
Ambient conditions
T_{ext} = 21.6 °C
T_{int}' = 20.5 °C



Coolant outlet temperatures for W1 spiral (above)



Pole-to-MPD heat flux



Coolant heat-removal fraction

CONCLUSIONS

Three operating regimes of the trim coil can be distinguished: excessive heat leakage at $Q_{pole} > Q^{max}$, acceptable heat leakage into the MPD inner volume at $0 < Q_{pole} < Q^{max}$, and heat inflow from the MPD inner air at $Q_{pole} < 0$. The excessive heat leakage was not observed under the provisional nominal parameters: Q_{pole} remained below Q^{max} = 300 W, reaching values up to 260 W. The parametric study showed that the thermal response is governed mainly by T_{inlet}: increasing T_{inlet} reduces the coolant heat-removal fraction ξ and increases Q_{pole}. For the West trim coil, currents up to the maximum applicable value indicate the onset of critical heat leakage at $I_W \approx 3.1$–3.8 kA; operation in this range would require additional thermal shielding. Increasing q from 19 to 21 L/min improves the thermal margin but does not remove the shielding requirement. Further work is focused on integrating the numerical model into the thermometry system for *in situ* calculation of the heat flux using data streamed from the experiment.